ChemComm

COMMUNICATION

View Article Online
View Journal

Cite this: DOI: 10.1039/c9cc04856a

Received 25th June 2019,
Accepted 15th August 2019

DOI: 10.1039/c9cc04856a

rsc.li/chemcomm

A versatile and accessible polymer coating for functionalizable zwitterionic quantum dots with high DNA grafting efficiency†

Chloé Grazon, ‡[ab] Margaret Chern, ‡[c] Katherine Ward, [d] Sébastien Lecommandoux, [a] Mark W. Grinstaff [bd] and Allison M. Dennis *[cd]

Efficient and versatile functionalization of poly(anhydride maleic-*alt*-isobutylene) (PIMA), with economical commercial reagents, results in the one-step/one-day production of a copper-free click chemistry-ready carboxybetaine-like coating for quantum dots (QDs). The QDs are bright and stable in aqueous media and easily grafted with DNA with >95% efficiency.

Quantum dots (QDs) are semiconductor nanoparticles with exceptional optical properties that are used in a variety of applications, including biosensing and biomedical imaging.[1] For such applications, QDs must be colloidally stable in aqueous media; however, the majority of QDs are synthesized in organic solvents and are not dispersible in water. Thus, strategies for imparting hydrophilicity to as-synthesized QDs are of keen interest.[2] Encapsulation methods provide bright and stable colloids, but significantly increase the nanoparticle hydrodynamic size (>20 nm), negatively impacting applications like single-QD tracking or histidine tag-mediated self-assembly of biomolecules on the nanoparticle surface.[3] Ligand exchange with a hydrophilic coating affords water dispersibility with a smaller final hydrodynamic radius (<20 nm), while multidentate ligands provide increased stability compared to monodentate ligands.[4]

Several groups describe multidentate polymer coatings[4c,5] consisting of (i) hydrophilic components such as poly(ethylene glycol) (PEG) or zwitterionic moieties and (ii) QD anchoring groups such as thiols or histidines.[6] PEG is the preferred steric coating for nanoparticles used in a biological environment, and zwitterionic compounds like sulfobetaine and carboxybetaine are garnering increased interest as they result in highly stable, non-fouling colloids.[7] For example, a charged QD surface coating developed by Mattoussi *et al.* uses poly(anhydride maleic-*alt*-isobutylene) (PIMA) as a backbone for easy functionalization with primary amines bearing imidazole, lipoic acid, and sulfobetaine moieties.[5d,e] While this method produces QDs that are small and bright, the synthesis of the zwitterionic sulfobetaine is multi-step and non-trivial (ESI,† Scheme S1). Alternatively, Lequeux *et al.* reported the use of commercially available monomers for synthesizing block copolymers poly(sulfobetaine methacrylate-*b*-vinyl imidazole) *via* RAFT polymerization, but the synthesis requires two steps and rigorous polymer characterization.[5b]

The availability of stable QD coatings that enable easy biofunctionalization is critical to the use and study of QDs by chemists and non-chemists alike. Here, we report a versatile single-step reaction to generate a multidentate, carboxybetaine-like polymer for coating QDs with a copper-free click chemistry handle for subsequent biofunctionalization. The straight forward method exclusively uses commercially available reagents and is suitable for the non-expert. We use this generalizable method to coat multiple QD compositions in a one-hour ligand exchange reaction. High efficiency (>95% yield) grafting of DNA to the polymer-coated QDs *via* copper-free click chemistry demonstrates the biofunctionalization potential, as controlled labeling of QDs with DNA is notoriously challenging.[8]

We prepared multiple compositions of heterostructured core/shell QDs following minor modifications to published protocols (ESI†) to demonstrate the generalizability of the coating method to a variety of colloidal QDs including CdSe and InP systems.[9] The multidentate polymer comprises a PIMA backbone, as reported by Mattoussi *et al.*,[5d,e] uniquely functionalized with a commercially available positive quaternary amine to counter the negative carboxylic acid created on each monomer during the amide formation, providing hydrophilicity through the generation of a carboxybetaine-like feature. Histamine anchors the polymer to the QD surface, and dibenzocyclooctyne (DBCO) provides a platform for subsequent copper-free click chemistry functionalization (Fig. 1A).[10] Using this polymer, we obtained water-dispersible QDs with excellent colloidal stability, grafting capability, and optical properties.

Successful polymer synthesis is confirmed by the formation of the amide bond resulting from the maleic anhydride-amine reaction *via* both ^{1}H NMR (Fig. S3–S8, ESI†) and IR spectroscopy. For all

[a] *Univ. Bordeaux, CNRS, Bordeaux INP, LCPO, UMR 5629, F-33600, Pessac, France*
[b] *Department of Chemistry, Boston University, Boston, MA, USA*
[c] *Division of Materials Science & Engineering, Boston University, Boston, MA, USA. E-mail: aldennis@bu.edu*
[d] *Department of Biomedical Engineering, Boston University, Boston, MA, USA*

† Electronic supplementary information (ESI) available: Material and methods, polymer and QD characterizations. See DOI: 10.1039/c9cc04856a

‡ These authors contributed equally.

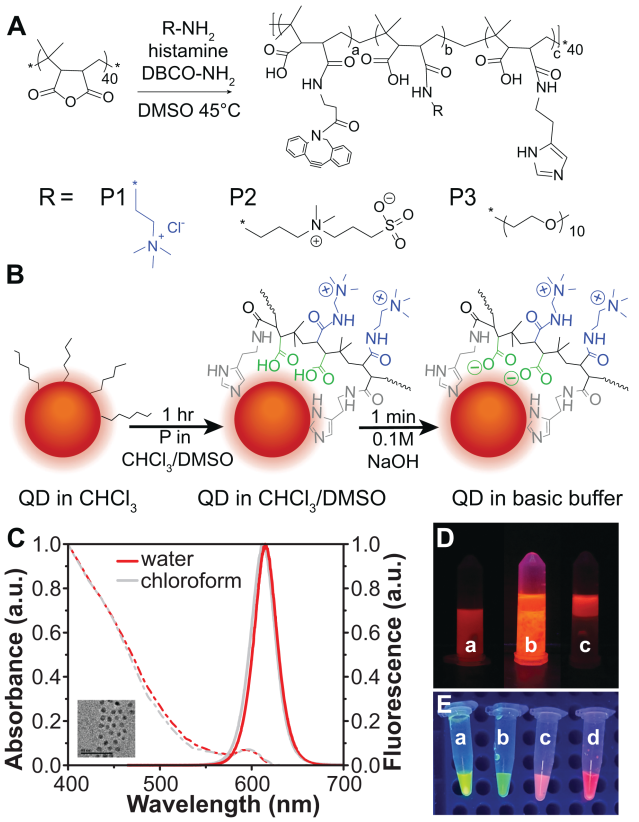

Fig. 1 (A) Schematic of the polymers used in this study and (B) of the ligand exchange protocol for QD@P1. (C) Absorption (dotted lines) and photoluminescence emission (solid lines) spectra (λ_{exc} = 400 nm) before (in $CHCl_3$) and after (in water) ligand exchange. Inset shows a representative TEM image of QDs@P1. Scale bar = 50 nm. (D) Image of CdSe based QDs during ligand exchange ((a) QD + P1 in $CHCl_3$, (b) addition of 0.1 M NaOH (c) successful transfer of QD@P1 from $CHCl_3$ to NaOH). (E) InP QDs of different emission wavelengths, size, and composition ligand transferred with P1 ((a) InP/7ZnSe/3ZnS, (b) InP/10ZnSe/3ZnS, (c) InP/3ZnS, (d) InP/2ZnSe/3ZnS).

polymers, the IR spectra (Fig. S9, ESI†) show the disappearance of the C=O stretch of the anhydride at 1770 cm^{-1} and appearance of the C=O stretch corresponding to the carboxylic acid and amide at 1710 cm^{-1} and 1650 cm^{-1}, respectively. Final polymer composition of P1, as evaluated by ^1H NMR in D_2O, consists of 39% histamines and 57% quaternary amine (Fig. S3, ESI†). Similar polymers possessing sulfobetaine (P2) and PEG_{550} (P3) for hydrophilicity are described for comparison. The reagents used for synthesizing P1 are significantly (~5-fold) less expensive than those used for P3. Furthermore, P1 only requires 1 day of synthesis to prepare, while P2 requires 7 days (Table S1, ESI†).

P3 is highly soluble both in aqueous and organic solvents like chloroform or THF, but P1 and P2 are only soluble in DMSO or water. Typically, as-synthesized QDs are soluble in non- to slightly polar organic solvents, making the QD and polymer solutions immiscible. Often, a two-step ligand exchange is used to address the solubility concern: QDs are first coated with a small, labile ligand (*e.g.*, mercaptopropionic acid),[5a] which is replaced by the polymer in an aqueous-phase ligand exchange. In contrast, ligand exchange with the PIMA-based polymers involves a simple one-step ligand exchange (Fig. 1B) with QDs and polymer mixed in a DMSO/$CHCl_3$ co-solvent. After an hour, the polymer-coated QDs are transferred into aqueous media by simply adding basic water to the solution (P1 and P2) or precipitating the QDs before recovery (P3); both methods produce bright and stable colloids. The optical and colloidal properties of CdSe/CdS/ZnS QDs coated with the different polymers for water dispersion exhibit similar properties. In all cases, the quantum yield is ~40% in chloroform and ~25% in water. QDs@P1 exhibit similar colloidal stability over time to QDs@P2 & P3 across a variety of pHs, salt concentrations, and temperatures, except at pH 5 where aggregation is more pronounced for P1 than P2 and P3 (Fig. S12, ESI†). After a week in dilute conditions at RT (50 nM QD, 1× HEPES), the fluorescence of the QDs remains unchanged (Fig. 2A). In contrast, QDs coated with the monomeric thioctic acid derivative CL4 (Scheme S2, ESI†)[11] precipitate after a week at RT (Fig. 2B and Fig. S12, ESI†). To highlight the generalizability of this approach, QDs of different compositions, size, and emission wavelength (InP/7ZnSe/3ZnS, InP/10ZnSe/3ZnS, InP/3ZnS, and InP/2ZnSe/3ZnS) were also phase transferred with P1 (Fig. 1E).

DLS of the polymer-coated QDs shows that all samples were of similar hydrodynamic diameter (~10 nm, Table S2 and Fig. S10, ESI†). Previous reports described his-tag self-assembly and Förster resonance energy transfer (FRET) with fluorescent proteins using QD@P2,[12] and we verify this function for P1 as well. A green emitting QD donor (one-pot CdSe/CdS/ZnS alloy, 10 nm diameter by TEM) was phase transferred using P1 and self-assembled with histidine-tagged tdTomato. The QD@P1 + tdTomato FRET pair exhibits acceptor sensitized emission and up to ~20% FRET efficiency (Fig. 2D and Fig. S13, ESI†), which

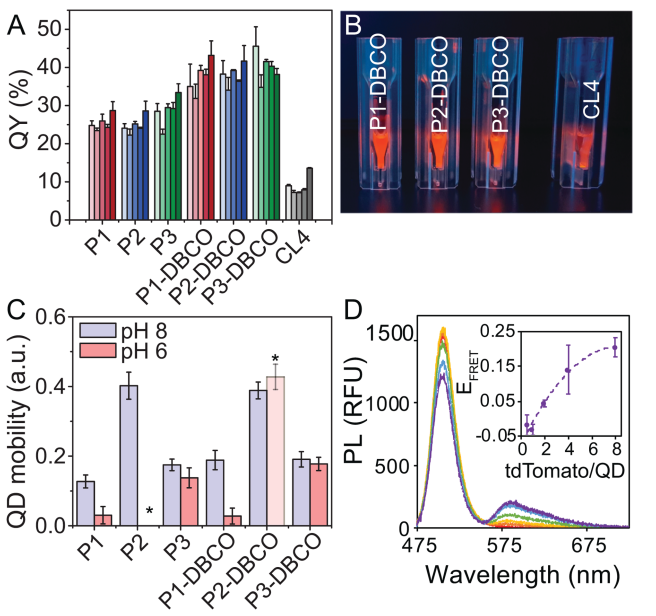

Fig. 2 (A) QY of the QDs after 1, 3, 4, 5 and 8 days (light to dark bars) of storage at RT in 1× HEPES. (B) Images of the QD solutions after storage for 8 days at RT in the dark. (C) Relative mobilities of QD@P run on a 1% agarose gel in 1× TAE buffer. *At pH6, QD@P2 had degraded and was not visible (data not shown). QD@P2-DBCO degrades as well, but enough fluorescence is retained to be seen (Fig. S11, ESI†). (D) PL spectra and FRET efficiency of the green QD@P1-tdTomato pair.

is reasonable given the large size of the donor (Table S3, ESI†), and demonstrates successful self-assembly.

Derivatives of PIMA with the zwitterion sulfobetaine (P2) or PEG (P3) are not neutral as each grafted amine introduces a carboxylic acid, adding an effective negative charge to the polymer at physiologic pH. The permanent positive charges provided by the quaternary amines on P1, however, balance the negative charges of the carboxylic acids on the backbone, creating a carboxybetaine-like polymer. We hypothesize that P1 will exhibit improved charge-neutrality compared to P2 and P3, although some negative surface charge will persist, as the addition of the histamines produces carboxylates that are not matched with positive charges. Zeta potential (ζ) measurements verify our hypothesis (Table S2, ESI†). The sulfobetaine-containing QD@P2 exhibits the most negative zeta potential ($\zeta = -36.0 \pm 1.5$ mV), while the carboxybetaine-like QD@P1 is most neutral ($\zeta = -12.7 \pm 2.0$ mV). The PEGylated QD@P3 ($\zeta = -18.1 \pm 0.9$ mV) is closer to neutral than QD@P2, likely due to PEG-based charge screening as previously seen in literature,[13] but still more negatively charged than QD@P1. This difference in surface charge is also evident in the gel mobility of the QDs, tested at pH 6 and 8 (Fig. 2 and Fig. S11, ESI†). At pH 8, the highly negatively charged QD@P2 moves the furthest; QD@P3 travels less than half as far, and the QD@P1 even less. At pH 6, QD@P1 exhibits minimal migration, indicating that some of its negatively charged carboxylates are protonated as the pH approaches their pK_a ($\sim$4.5), reducing the excess negative charge. QD@P2 loses fluorescence or degrades at pH 6, as it is no longer visible in the fluorescent image of the gel, while the migration of QD@P3 is the same at both pHs. None of the migration patterns change significantly with the addition of DBCO functionality.

The inclusion of DBCO for strain-promoted alkyne-azide cycloaddition (SPAAC) functionalization facilitates applications in biology and medicine. Using copper-free click chemistry to graft azido-functionalized entities to the PIMA-coated QDs is preferred over conventional copper-catalyzed click chemistry on QDs, as the presence of residual copper may reduce QD fluorescence.[14] We prepared QD analogs of P1–P3 with $\sim$10% DBCO using the protocols described above. All QD@P-DBCO samples exhibit significantly higher QY compared to polymer coatings without DBCO (40% *vs.* 25%, respectively). We suspect that the hydrophobic nature of DBCO allows for: (i) increased solubility of the polymer in the organic solvents, minimizing the chance for aggregation during ligand exchange; and/or (ii) improved anchoring of the polymer on the QD surface potentially providing better protection of the QD from water. All the QDs with DBCO are as stable as their DBCO-free counterparts, and their surface charge shows the same trend, with QD@P1-DBCO being the most neutral (Fig. 2 and Fig. S11, Table S2, ESI†). The number of DBCO handles and PIMA strands per QD are estimated by measuring the DBCO absorbance in the UV (ε_{309} = 12 000 M^{-1} cm^{-1}) of cleaned QD@P-DBCOs (Fig. S14 and Table S4, ESI†) and relating the DBCO absorbance to the DBCO/polymer ratio determined by NMR. On average, QD@P1-DBCO is coated with 15 polymer chains, QD@P2-DBCO with 30, and QD@P3-DBCO with 95 after multiple buffer exchange steps with 100 kDa centrifugal filtration devices to remove excess polymer. The ligand exchange reactions are highly reproducible, as replicate QD–DBCO preparations produced very similar polymer/QD ratios (Table S4, ESI†). We hypothesize that the amphiphilic nature of P3-DBCO may result in the formation of multiple polymer layers around the QD, increasing the number of polymer strands per QD. Filtration efficiency of random coil polymers can vary when compared to more compact species of similar molecular weight, which may also affect the final polymer/QD ratios obtained.

To demonstrate the utility of the SPAAC-ready coating, we grafted 5′-azide-functionalized single-stranded DNA (DNA-N_3) to DBCO-functionalized QDs. Examples of DNA grafting to QD surface ligands have been reported[8] using traditional biochemistries like amine–carboxylic acid[15] or thiol–maleimide[16] reactions, but the percentage of DNA strands conjugated rarely exceed 50%. Previous alkyne–azide click chemistry QD–DNA grafting methods exhibited up to 67% efficiency.[5c,12,17] For DNA labeling, we simply mix QD@P-DBCO with DNA-N_3 (Table S5, ESI†) for 4 days in the dark at pH 8.6 (0.1 M $NaHCO_3$) with 1 M NaCl (Fig. 3). The high salt concentration screens the charges between QD@P-DBCO and DNA and improves grafting efficiency.[15,16]

The QD–DNA conjugates were analyzed on agarose gels stained with SYBR green for ssDNA detection (Fig. 3B). Using a filter to remove red QD fluorescence facilitated acquisition of DNA-only and QD + DNA gel images to visualize colocalization (Fig. S15, ESI†). In reactions with a molar excess of DBCO (*e.g.*, for P1, QD/DBCO/DNA = 1/55/20, Table S6, ESI†), no free DNA is observed for any of the QD@P-DBCO polymers; DNA fluorescence completely colocalizes

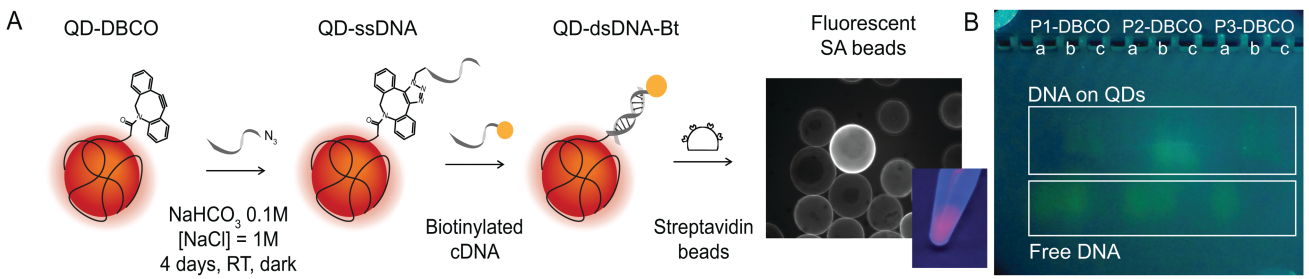

Fig. 3 (A) Schematic of the copper-free click reaction between QD@P-DBCO + DNA-N_3 and hybridization of the QD–ssDNA with its biotinylated complement. The QD–dsDNA-bt can be pulled down on streptavidin (SA) beads to verify hybridization. (B) Image of a 1% agarose gel in 1× TBE buffer stained with Sybr Green. QD fluorescence removed with a 500 nm short-pass filter to visualize the DNA by itself. All QD@P-DBCO are loaded at the same concentration in the same reaction conditions: (a) QD@P-DBCO + 20× DNA-NH_2 (negative control); (b) QD@P-DBCO + 50× DNA-N_3; (c) QD@P-DBCO + 20× DNA-N_3.

with QD fluorescence. When using QD@P3-DBCO, the DNA band is slightly offset from the QD band. In light of the high polymer/QD ratios discussed above, we attribute this to excess polymer that is not directly anchored to the QD surface desorbing during gel electrophoresis. Analysis of QD@P1-DBCO with ImageJ shows that more than 95% of the initial DNA-N_3 is grafted on the QD (Fig. S15 and S16, ESI†). Aggregation of QD@P1-DBCO in the control reactions is evident as some QDs remain trapped in the loading well of the gel, likely a result of the high salt conditions of the click reaction (Fig. 3 and Fig. S15, S16, ESI†). When DNA is conjugated to the QD@P1-DBCO, the DNA appears to impart additional stability and no aggregation is observed, indicating the potential for simple centrifugation-based removal of unlabeled QDs when using P1-DBCO. QD@P2&3-DBCO did not exhibit this behavior. When using larger QD/DNA ratios (QD/DBCO/DNA = 1/55/50), ImageJ analysis indicates 80% reaction efficiency for QD@P1-DBCO. To our knowledge, the >95% DNA grafting efficiency obtained for QD@P1-DBCO is the highest reported on QDs. For most downstream applications, <5% free DNA would not warrant further purification, once again improving the overall yield and duration of the reaction.

Lastly, we confirm that the conjugated ssDNA is available for hybridization. QD@P1-DBCO–DNA hybridizes with a biotinylated complementary strand with 61% efficiency (QD–DNA-bt, Tables S3 and S7, ESI†). Upon mixing the QD–dsDNA conjugate with streptavidin-coated agarose beads and washing away unbound QDs, imaging with a fluorescent microscope reveals agarose beads decorated with the QD–DNA-bt (Fig. 3). Control experiments with QD@P1-DBCO–DNA hybridized with the non-biotinylated DNA and QD@P1-DBCO (no DNA) mixed with biotinylated dsDNA–biotin do not exhibit fluorescence, indicating that there is no non-specific adsorption of the QD@P1-DBCO to the beads (Fig. S17, ESI†).

In conclusion, we report the synthesis of an easy, fast, and inexpensive polymer for obtaining stable and bright QDs in water. The use of commercially available reagents in an accessible procedure enables a wider variety of research groups to fabricate zwitterionic QDs. When used for the QD phase exchange procedure, the mixed positive and negative charge of the carboxybetaine-like P1 polymer provides for excellent QD colloidal and optical properties. We incorporate a DBCO handle to enable passive biofunctionalization of the coated QDs. We demonstrate the advantages of the conjugation approach by grafting the QDs with azide-functionalized DNA with >95% efficiency. Given the advantages of this zwitterionic polymer, the single-step QD coating procedure, and high grafting efficiency, we encourage others to use this polymer to synthesize functional or responsive QDs for *in vitro* and *in vivo* biosensing and biomedical imaging applications.

CG received support from a Marie-Curie fellowship from the European Union under the program H2020, Grant 749973 and acknowledges Dr A. Badon for his help on the multicolor imager set-up. Financial support for MC was provided through the Clare Boothe Luce (CBL) Graduate Fellowship from the Henry Luce Foundation. AMD was supported by the National Center for Advancing Translational Sciences, National Institutes of Health, through BU-CTSI Grant Number 1KL2TR001411. This work was also performed in part at the Center for Nanoscale Systems (CNS), a member of the National Nanotechnology Infrastructure Network (NNIN), which is supported by the National Science Foundation under NSF award no. ECS-0335765. CNS is part of Harvard University.

Conflicts of interest

There are no conflicts to declare.

Notes and references

1 (*a*) M. Chern, J. C. Kays, S. Bhuckory and A. M. Dennis, *Methods Appl. Fluoresc.*, 2019, **7**, 012005; (*b*) J. Zhou, Y. Yang and C.-y. Zhang, *Chem. Rev.*, 2015, **115**, 11669–11717.
2 (*a*) A. S. Karakoti, R. Shukla, R. Shanker and S. Singh, *Adv. Colloid Interface Sci.*, 2015, **215**, 28–45; (*b*) K. E. Sapsford, W. R. Algar, L. Berti, K. B. Gemmill, B. J. Casey, E. Oh, M. H. Stewart and I. L. Medintz, *Chem. Rev.*, 2013, **113**, 1904–2074.
3 (*a*) F. Pinaud, S. Clarke, A. Sittner and M. Dahan, *Nat. Methods*, 2010, **7**, 275; (*b*) A. M. Dennis, D. C. Sotto, B. C. Mei, I. L. Medintz, H. Mattoussi and G. Bao, *Bioconjugate Chem.*, 2010, **21**, 1160–1170.
4 (*a*) N. Zhan, G. Palui, M. Safi, X. Ji and H. Mattoussi, *J. Am. Chem. Soc.*, 2013, **135**, 13786–13795; (*b*) H. T. Uyeda, I. L. Medintz, J. K. Jaiswal, S. M. Simon and H. Mattoussi, *J. Am. Chem. Soc.*, 2005, **127**, 3870–3878; (*c*) M. Sun, L. Yang, P. Jose, L. Wang and J. Zweit, *J. Mater. Chem. B*, 2013, **1**, 6137–6146.
5 (*a*) E. Giovanelli, E. Muro, G. Sitbon, M. Hanafi, T. Pons, B. Dubertret and N. Lequeux, *Langmuir*, 2012, **28**, 15177–15184; (*b*) M. Tasso, E. Giovanelli, D. Zala, S. Bouccara, A. Fragola, M. Hanafi, Z. Lenkei, T. Pons and N. Lequeux, *ACS Nano*, 2015, **9**, 11479–11489; (*c*) L. Ma, C. Tu, P. Le, S. Chitoor, S. J. Lim, M. U. Zahid, K. W. Teng, P. Ge, P. R. Selvin and A. M. Smith, *J. Am. Chem. Soc.*, 2016, **138**, 3382–3394; (*d*) W. Wang, A. Kapur, X. Ji, M. Safi, G. Palui, V. Palomo, P. E. Dawson and H. Mattoussi, *J. Am. Chem. Soc.*, 2015, **137**, 5438–5451; (*e*) N. Zhan, G. Palui and H. Mattoussi, *Nat. Protoc.*, 2015, **10**, 859.
6 M. A. Boles, D. Ling, T. Hyeon and D. V. Talapin, *Nat. Mater.*, 2016, **15**, 141.
7 (*a*) C. Leng, H.-C. Hung, S. Sun, D. Wang, Y. Li, S. Jiang and Z. Chen, *ACS Appl. Mater. Interfaces*, 2015, **7**, 16881–16888; (*b*) W. Yang, S. Liu, T. Bai, A. J. Keefe, L. Zhang, J.-R. Ella-Menye, Y. Li and S. Jiang, *Nano Today*, 2014, **9**, 10–16.
8 A. Banerjee, T. Pons, N. Lequeux and B. Dubertret, *Interface Focus*, 2016, **6**, 20160064.
9 (*a*) M. Chern, T. T. Nguyen, A. H. Mahler and A. M. Dennis, *Nanoscale*, 2017, **9**, 16446–16458; (*b*) R. Toufanian, A. Piryatinski, A. H. Mahler, R. Iyer, J. A. Hollingsworth and A. M. Dennis, *Front. Chem.*, 2018, **6**, 567; (*c*) W. K. Bae, K. Char, H. Hur and S. Lee, *Chem. Mater.*, 2008, **20**, 531–539.
10 J. C. Jewett and C. R. Bertozzi, *Chem. Soc. Rev.*, 2010, **39**, 1272–1279.
11 K. Susumu, E. Oh, J. B. Delehanty, J. B. Blanco-Canosa, B. J. Johnson, V. Jain, W. J. Hervey, W. R. Algar, K. Boeneman, P. E. Dawson and I. L. Medintz, *J. Am. Chem. Soc.*, 2011, **133**, 9480–9496.
12 W. Wang, X. Ji, A. Kapur, C. Zhang and H. Mattoussi, *J. Am. Chem. Soc.*, 2015, **137**, 14158–14172.
13 C. Grazon, J. Rieger, P. Beaunier, R. Méallet-Renault and G. Clavier, *Polym. Chem.*, 2016, **7**, 4272–4283.
14 A. Bernardin, A. Cazet, L. Guyon, P. Delannoy, F. Vinet, D. Bonnaffé and I. Texier, *Bioconjugate Chem.*, 2010, **21**, 583–588.
15 D. Sun and O. Gang, *Langmuir*, 2013, **29**, 7038–7046.
16 A. Banerjee, C. Grazon, B. Nadal, T. Pons, Y. Krishnan and B. Dubertret, *Bioconjugate Chem.*, 2015, **26**, 1582–1589.
17 (*a*) H. Zhang, G. Feng, Y. Guo and D. Zhou, *Nanoscale*, 2013, **5**, 10307–10315; (*b*) L. Trapiella-Alfonso, T. Pons, N. Lequeux, L. Leleu, J. Grimaldi, M. Tasso, E. Oujagir, J. Seguin, F. d'Orlyé, C. Girard, B.-T. Doan and A. Varenne, *ACS Appl. Mater. Interfaces*, 2018, **10**, 17107–17116; (*c*) W. Wang, A. Kapur, X. Ji, B. Zeng, D. Mishra and H. Mattoussi, *Bioconjugate Chem.*, 2016, **27**, 2024–2036; (*d*) J. Hao, L.-L. Huang, R. Zhang, H.-Z. Wang and H.-Y. Xie, *Anal. Chem.*, 2012, **84**, 8364–8370.

